Nanoscale

Tuning the Seebeck coefficient of naphthalenediimide by electrochemical gating and doping.

Journal:	*Nanoscale*
Manuscript ID	NR-ART-01-2017-000571.R1
Article Type:	Paper
Date Submitted by the Author:	19-Feb-2017
Complete List of Authors:	Al-Galiby, Qusiy; Lancaster University, Physics Sadeghi, Hatef; Lancaster University, Physics Manrique, David; Lancaster University Lambert, Colin; Lancaster University, Physics

Dear Professor Guldi,

Many thanks for the reviewers' comments on our manuscript "*Tuning the Seebeck coefficient of naphthalenediimide by electrochemical gating and doping*." We appreciate their careful comments and have used these to improve the manuscript. In our detailed reply below, all additions to the manuscript are shown in yellow.

Best regards,

Colin Lambert

Reply to Reviewer comments:

REVIEWER REPORT(S):
Referee: 1

Comments to the Author
This is a computational paper exploring the thermoelectric properties of single molecule nathpthalenediimide derivative connected to 2 gold electrode through benzothiophene. They investigate electrogating and doping. Doping with TTF is especially relevant for practical applications. The authors have experience studying this system, see Y. Li, M. Baghernejad, Q. Al-Galiby, D. Manrique, G. Zhang, J. Hamill, Y. Fu, P. Broekmann, W. Hong, T. Wandlowski, D. Zhang, C. J. Lambert "A Three State NDI Switch: Integration of Pendant Redox Unit for Conductance Tuning" Condensed Matter e print submitted 8 Nov 2016
arXiv:1611.02725 [cond-mat.mes-hall]. The work is novel and, if correct, would have a high impact on the field of thermoelectric materials. However, this reviewer is unsure about the methods used to evaluate the thermoelectric properties and how the computational work predicts experimental data. Also, this reviewer would have appreciated hypotheses to explain their results.

Comment: First, they switch between neutral, radical and di-anion states using electrochemical doping. Surprisingly, the sign of Seebeck coefficient becomes positive for the radical and di-anion states. This reviewer would have expected negative Seebeck coefficient as the molecule becomes more negatively charged. Can the authors explain this phenomena? Any insights? How is their method of calculating Seebeck coefficient relevant to real experimental experiments and real materials? Could the authors validate their data? i.e. compare with known experimental data? Are the absolute numbers relevant or should we only look at relative trends?
Reply:
If the Fermi energy is initially near the middle of the HOMO-LUMO gap, then indeed a negative Seebeck coefficient S is expected as the molecule becomes more negatively charged and the LUMO moves closer to the Fermi energy. For example in figure S2a, if the LUMO decreased in energy by no more than 0.1 eV, then S would become more negative. However such a shift involves only a small change in the charge on the molecule. Changing the redox state such that the NDI gains one or two electrons creates a much more significant change in the electronic structure of the molecule. For example comparison between figures S2a and S2c shows that the original LUMO completely passes below the Fermi energy, thereby changing the slope of the transmission function from positive to negative and S from negative to positive. This significant change in electronic structure has been experimentally verified by the order of magnitude differences between the measured conductances of the three redox states (see above mentioned ref which is cited as ref 22 of the main text).

We believe our method of calculating Seebeck coefficient relevant to real experimental experiments and real materials, because as mentioned above, we have experience studying this system, and have benchmarked our DFT calculations against the above-mentioned experimental measurements of the electrical conductance of the neutral, radical and di-anion states. Crucially, this benchmarking allows us to pin down the Fermi energy E_F and therefore to obtain the Seebeck coefficient from the slope of the transmission curves at E_F. In our other recent studies such as (L.Rincón-García, A. K. Ismael, C. Evangeli,I. Grace,G.Rubio-Bollinger,K. Porfyrakis, N. Agraït& C. J. Lambert, Nature Materials 15, 289–293 (2016)) it has been experimentally demonstrated that our theoretical approach can predict both the conductance and the Seebeck coefficient. For this reason, we have confidence in the absolute numbers.

To address this point, the following text has been added to the end of the paragraph just above figure 3 of the main text.

It is interesting to note that if the Fermi energy is initially near the middle of the HOMO-LUMO gap, then a negative Seebeck coefficient *S* is expected as the molecule becomes more negatively charged and the LUMO moves closer to the Fermi energy. For example in figure S2a, if the LUMO decreased in energy by no more than 0.1 eV, then *S* would become more negative. However such a shift involves only a small change in the charge on the molecule. Changing the redox state such that the NDI gains one or two electrons creates a much more significant change in the electronic structure of the molecule. For example comparison between figures S2a and S2c shows that the original LUMO completely passes below the Fermi energy, thereby changing the slope of the transmission function from positive to negative and *S* from negative to positive. This significant change in electronic structure has been experimentally verified by the order of magnitude differences between the measured conductances of the three redox states[22].

Comment:
Second, the authors optimize thermoelectric properties with doping, which is more practical and relevant. It is known that doping allows for optimization of thermoelectric properties. E.g. increases charge carrier and thus electrical conductivity. Doping with TTF (electron donor) increased Seebeck coefficient (became more negative). While the sign is as expected for n-type organic semiconductor, the fact that it increased with doping is opposite to general trend observed for organic semiconductors. (e.g. Kroon, R.; Mengistie, D. A.; Kiefer, D.; Hynynen, J.; Ryan, J. D.; Yu, L.; Muller, C., Thermoelectric plastics: from design to synthesis, processing and structure-property relationships. 2016, 45, 6147-6164.) Can the authors provide any physical insights or explanation for their results?

Reply:

In fact high-Seebeck coefficients after n-doping are not unprecedented in organic semiconductors. In the above review, it is noted that Schlitz *et al.* demonstrated that n-doping of napthalenedicarboximide-bithiophene copolymer P(NDIOD-T2)leads to a high negative Seebeck coefficient of –850 μV K^{-1}. The main explanation is that the Fermi energy of the undoped molecules should be far from the LUMO, so that n-doping causes the Fermi energy to sit closer to the LUMO, in a region of a steep slope for the transmission function. This behaviour is shown in figure 5, where doping with TTF causes the energy levels of the NDI to decrease in energy and therefore the LUMO resonance moves closer to the Fermi energy, leading to an increase in the slope and hence to a more negative Seebeck coefficient at low temperatures, as shown in figure 6b.

To address this point, we have included the above references and added the following text to the paragraph above table 1:

High-Seebeck coefficients after n-doping are not unprecedented in organic semiconductors. For example[28], Schlitz *et al.*[29] demonstrated that n-doping of napthalenedicarboximide-bithiophene copolymer P(NDIOD-T2) leads to a high negative Seebeck coefficient of –850 $\mu V\ K^{-1}$.

28 R. Kroon, D.A. Mengistie, D. Kiefer, J. Hynynen, J.D. Ryan, L. Yu, C. Muller, C., *Chem. Soc. Rev.* 2016, **45**, 6147-6164

29 R. A. Schlitz, F. G. Brunetti, A. M. Glaudell, P. Levi Miller, M. A. Brady, C. J. Takacs, C. J. Hawker and M. L. Chabinyc, Adv. Mater. 2014, **26**, 2825–2830

Comment:
Other details:
Figure 4 color code in legend does not match figure.

Reply:

Referee: 2 Many thanks for spotting this typo. We have now amended the legend.

Comments to the Author
In this manuscript, Lambert and coworkers demonstrated that switching between the neutral, radical and di-anion charge states of NDI, their molecular energy levels relative to the Fermi energy of the electrodes can be swapped. This is expected, but was demonstrated first time by the authors with experimental evidence and theoretical justification.

Reply.

We thank the reviewer for these encouraging comments.

Tuning the Seebeck coefficient of naphthalenediimide by electrochemical gating and doping.

Qusiy H. Al-Galiby,[a,b*] Hatef Sadeghi, [a] David Zsolt Manrique,[c] and Colin J. Lambert[a*]

[a]Department of Physics, Lancaster University, Lancaster LA1 4YB, United Kingdom.
[b]Department of Physics, Education of College, Al Qadisiyah University, IRAQ.
[c]Department of Electronic & Electrical Engineering - Photonics Group, University College London,UK

*Corresponding author: c.lambert@lancaster.ac.uk and qusiy.algaliby@qu.edu.iq
Electronic Supplementary Information (ESI) available. See DOI: 10.1039/b000000x/

Abstract

We investigate the sign and magnitude of the single-molecule Seebeck coefficient of naphthalenediimide (NDI) under the influence of electrochemical gating and doping. The molecule consists of a NDI core with two alkyl chains in the bay-area position, connected to gold electrodes via benzothiophene (DBT) anchor groups. By switching between the neutral, radical and di-anion charge states, we are able to tune the molecular energy levels relative to the Fermi energy of the electrodes. The resulting single-molecule room-temperature Seebeck coefficents of the three charge states are -294.5 μv/K, 122 μv/K and 144 μv/K respectively and the room-temperature power factors are 4.4×10^{-5} W/m.K^2 , 3×10^{-5} W/m.K^2 and 8.2×10^{-4} W/m.K^2. As a further strategy for optimising thermoelectric properties, we also investigate the effect on both phonon and electron transport of doping the NDI with either an electron donor (TTF) or an electron acceptor (TCNE). We find that doping by TTF increases the room-temperature Seebeck coefficient and power factor from -73.7 μv/K and 2.6×10^{-7} W/m.K^2 for bare NDI to -105 μv/K and 3.6×10^{-4} W/m.K^2 in presence of TTF. The low thermal conductance of NDI-TTF, combined with the higher Seebeck coefficient and higher electrical conductance lead to a maximum thermoelectric figure of merit of ZT = 1.2, which is higher than that of bare NDI in several orders of magnitude. This demonstrates that both the sign and magnitude of NDI Seebeck coefficient can be tuned reversibly by electrochemical gating and doping, suggesting that such redox active molecules are attractive materials for ultra-thin-film thermoelectric devices.

1. Introduction

The Seebeck effect can be used to create electricity from a variety of sources of waste heat such as data farms and automobile exhausts and the inverse process (i.e. the Peltier effect) can be exploited in cascade coolers for on-chip cooling of electronic devices[1–3]. However the more widespread application of these effects is limited by the poor performance of available materials[1] and therefore research aimed at identifying the parameters that control the efficiency of thermoelectric materials is intensifying[4–11]. One approach involves exploiting the room-temperature properties of single-molecules attached to nanogap electrodes and identifying strategies for controlling their thermoelectric properties[12,13]. Since the Seebeck coefficient of inorganic nanostructures such as nanotubes, nanowires and nanodots can be tuned by electrostatic gating[14–21], it is natural to explore the response of organic single-molecule junctions to an external electric field, induced by electrochemical gating or charge transfer complexation with dopants. For this purpose, redox-active molecules such as

viologen or naphthalenediimide (NDI) (fig. 1) are attractive candidates, since their charge state can be changed with a relatively-low electrochemical potential[22]. From the point of view of optimising thermoelectric properties, junctions formed from such molecules are of interest, because by controlling the number of electrons on the molecule, it should be possible to tune the molecular energy levels relative to the Fermi energy E_F of the electrodes[23], leading to transport resonances, which enhance the thermopower. In what follows, we shall demonstrate that this is indeed the case and that large positive and negative thermopowers are achievable. On the other hand, although electrochemical gating is an interesting research tool for probing transport properties, it is not useful for the purpose of creating high-performance thermoelectric devices formed from molecular films, since the electrochemical environment would conductance heat and reduce the efficiency of the film. Therefore after demonstrating the efficacy of electrochemical gating, we proceed to examine the effect of doping by the electron donor TTF and the electron acceptor TCNE and demonstrate that doping is a viable route to large Seebeck coefficients and large thermoelectric efficiencies.

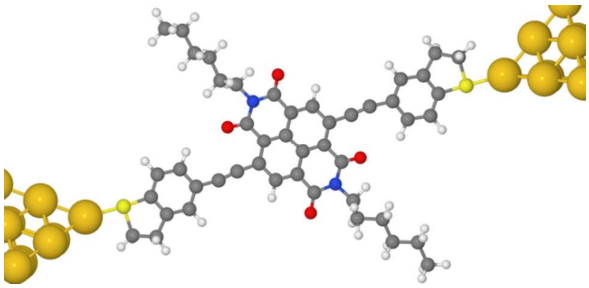

Figure 1. An optimized single-molecule junction formed from a NDI molecule attached to gold electrodes.

To model the effect of electrochemical gating, the charge state of the NDI molecule was controlled by introducing a charge double layer (CDL) in the vicinity of the NDI backbone, as shown in Figure 2. In the absence of the CDL, the NDI possesses a small negative charge and therefore as shown in Figure 2a, to induce the charge-neutral state the negative charges of the CDL dipoles point towards the NDI backbone. The radical anion and di-anion states are then produced by reversing the CDL dipoles and adjusting the average distance y of the closest CDL ions from the NDI backbone.

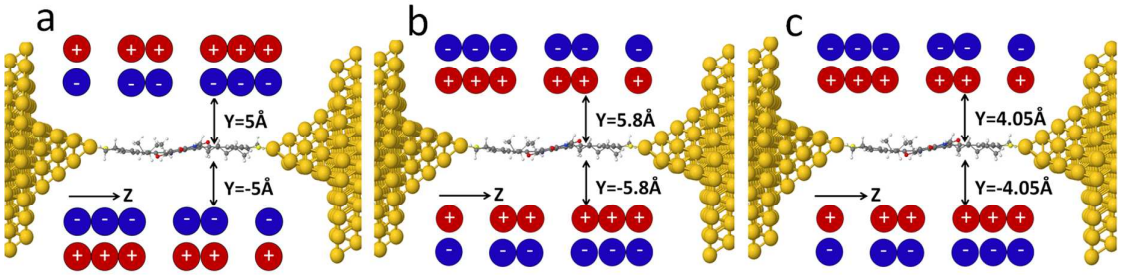

Figure 2. Junction geometries with charge double layers (CDLs) corresponding to three charge states of the NDI: (a) the neutral state (b) the radical anion and (c) the radical di-anion state.

To model the fluctuating environment encountered by molecules in the presence of a CDL, results were obtained for several different CDL arrangements, in which the anions and cations were randomly arranged at a fixed distance y. For each choice of *y*, the transmission coefficient $\boldsymbol{T^{\sigma}(E)}$ for electrons of energy $\boldsymbol{E}$, spin $\boldsymbol{\sigma}$ = [↑, ↓] passing through the molecule from one electrode to the other was calculated from which the electrical conductance, Seebeck coefficient were obtained (see Methods). If the electrical conductance and Seebeck coefficient for the *i*th CDL arrangement are denoted $\boldsymbol{G_i}$ and $\boldsymbol{S_i}$ respectively, then two distinct ensemble-averaged Seebeck coefficients are of interest, which we denote $\boldsymbol{< S >}$ and $\boldsymbol{\overline{S}}$. The first is the straightforward average Seebeck coefficient $\boldsymbol{< S >= (1/N)\sum_i S_i}$, where $\boldsymbol{N}$ is the number of CDL arrangements. The second is a "conductance-weighted ensemble average," given by $\boldsymbol{\overline{S} =< GS >/< G >}$. As discussed in[24], $\boldsymbol{\overline{S}}$ is the relevant quantity when using single-molecule Seebeck coefficients to estimate the Seebeck coefficient of a dilute thin film of such molecules. For each of the three NDI charge states, Figures 3a-c show the average conductance $\boldsymbol{< G >}$, the average Seebeck coefficient $\boldsymbol{< S >}$ and conductance-weighted Seebeck coefficient $\boldsymbol{\overline{S}}$ as functions of temperature, obtained using the DFT-predicted Fermi energy $\boldsymbol{E_F^{DFT}}$ (see Methods). The computed trend in $\boldsymbol{< G >}$ (Fig 3c) agrees well with experimental measurements[22], whereas there exist currently no measurements for $\boldsymbol{< S >}$ and $\boldsymbol{\overline{S}}$. Figure 3a shows that both the sign and magnitude of the average thermopower $\boldsymbol{\overline{S}}$ are sensitive to the charge state of the NDI, taking room-temperature values of -295 μV/K, +122 μV/K and +144 μV/K for the neutral, anion and di-anion states respectively. It is interesting to note that if the Fermi energy is initially near the middle of the HOMO-LUMO gap, then a negative Seebeck coefficient *S* is expected as the molecule becomes more negatively charged and the LUMO moves closer to the Fermi energy. For example in figure S2a, if the LUMO decreased in energy by no more than 0.1 eV, then *S* would become more negative. However such a shift involves only a small change in the charge on the molecule. Changing the redox state such that the NDI gains one or two electrons creates a much more significant change in the electronic structure of the molecule. For example comparison between figures S2a and S2c shows that the original LUMO completely passes below the Fermi energy, thereby changing the slope of the transmission function from positive to negative and *S* from negative to positive. This significant change in electronic structure has been experimentally verified by the order of magnitude differences between the measured conductances of the three redox states[22].

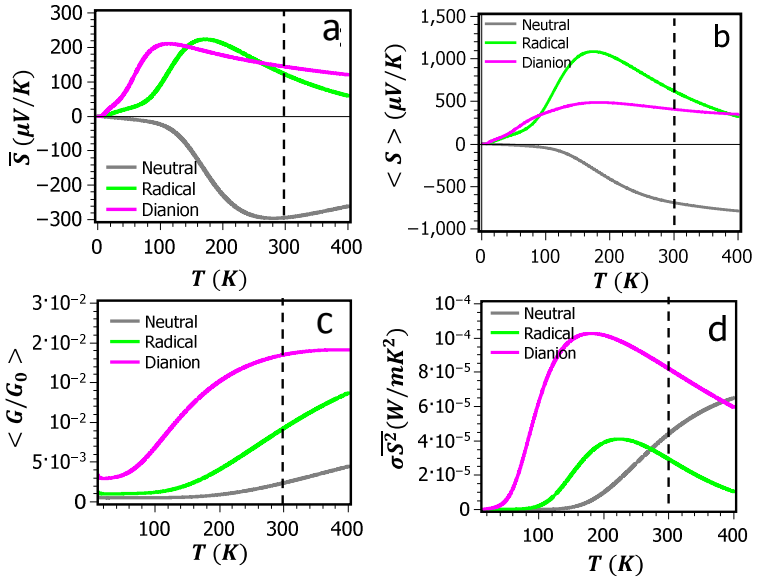

Figure 3. 3a, 3b and 3c show the averaged quantities $\overline{\boldsymbol{S}}$, $< \boldsymbol{S} >$ and $< \boldsymbol{G} >$ respectively for junction geometries with double layers located at distances y=5Å, y=5.8Å and y=4.05Å. Figure 3d shows the corresponding power factor $\boldsymbol{\sigma\overline{S}^2}$. All quantities are plotted as a function of temperature and obtained using the DFT-predicted Fermi energy $\boldsymbol{E_F^{DFT}}$. The colour code refers to the three different states, NDI-N (grey), NDI-R (green) and NDI-D (pink).

A crucial quantity determining the efficiency of a bulk thermoelectric material is the dimensionless figure of merit $\boldsymbol{ZT = PT/\kappa}$, where $\boldsymbol{P = \sigma\overline{S}^2}$ is the power factor, $\boldsymbol{\sigma}$ is the electrical conductivity and $\boldsymbol{\kappa}$ is the thermal conductivity due to both phonons and electrons. In an electrochemical environment, $\boldsymbol{ZT}$ is not relevant, because $\boldsymbol{\kappa}$ will be determined by heat flows through the electrochemical medium. However the numerator of $\boldsymbol{ZT}$ (i.e. the power factor $\boldsymbol{P}$) is of interest.

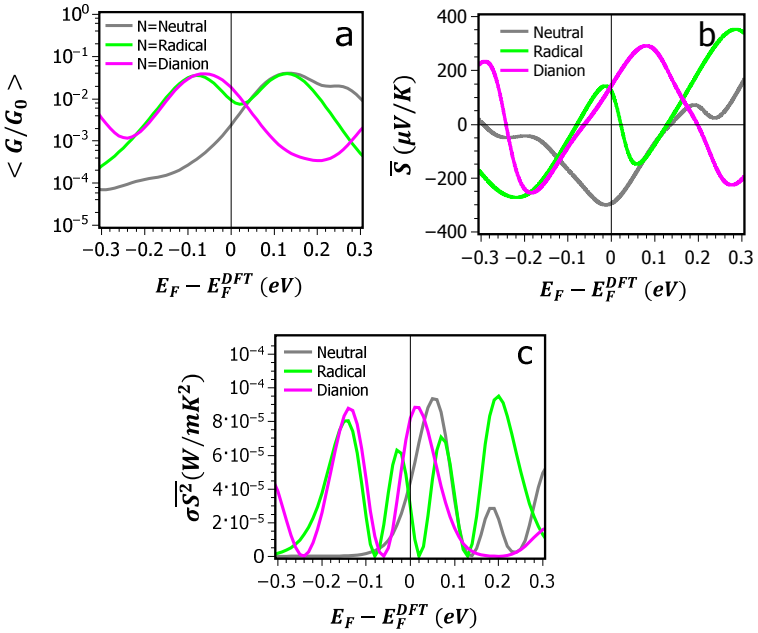

Figure 4. (a, b and c) show The room-temperature ensemble-averaged electrical conductances $< \boldsymbol{G} >$, thermopower $\overline{\boldsymbol{S}}$ and power factor $\boldsymbol{\sigma\overline{S}^2}$ plotted for a range of Fermi energies E_F relative to the DFT-predicted

Fermi energy E_F^{DFT} for each NDI charge state. The grey curve shows the neutral state, the green curve is the anion state and the magenta curve is the di-anion state.

The notion of conductivity is not applicable to transport through single molecules, but to compare with literature values for bulk materials, we define $\boldsymbol{\sigma} = < \boldsymbol{G} > \boldsymbol{L}/\boldsymbol{A}$, where $\boldsymbol{L}$ and $\boldsymbol{A}$ are equal to the length and the cross-sectional area of the molecule respectively. Using the values $\boldsymbol{L}$=3.6 nm and $\boldsymbol{A}$=1.4 nm^2 yields the results in Figure 3d, which show that at low temperature, the anion and di-anion states have the highest power factors. The room-temperature power factors of between 20 and 80 μW/m.K^2 compare favourably with power factors of other organic materials, whose reported values range from 0.016 μW/m.K^2 and 0.045 μW/m.K^2 for Polyaniline and Polypyrole respectively[25], to 12 μW/m.K^2 for PEDOT:PSS[26] and (12μW/m.K^2 for C60/Cs2Co3 Dph-BDT[27].

Figure 4a, 4b and 4c 5d show results for the room-temperature ensemble-averaged electrical conductances $< \boldsymbol{G} >$, Seebeck coefficient (thermopower) $\overline{\boldsymbol{S}}$ and power factor $\boldsymbol{\sigma}\overline{\boldsymbol{S}}^{\boldsymbol{2}}$. It is well-known that DFT can give inaccurate value for the Fermi energy and therefore Figures 4a, 4b and 4c show corresponding results for a range of Fermi energies E_F relative to the DFT-predicted Fermi energy E_F^{DFT}.

Although control of thermoelectric properties by electrochemical gating is a versatile research tool for fundamental studies, parasitic heat conduction by the electrolyte means that the resulting *ZT* would be low. To avoid this feature, we now study how phonon and electron transport can be tuned using charge transfer complexation with the electron donor TTF and the acceptor TCNE.

Fig 5a shows an example of NDI complexed with TTF, whose electron transmission coefficient (blue curve in Fig 5b) leads to the room-temperature electrical conductance shown in Fig 5c (blue curve). For comparison, the red curves show corresponding results for bare NDI.

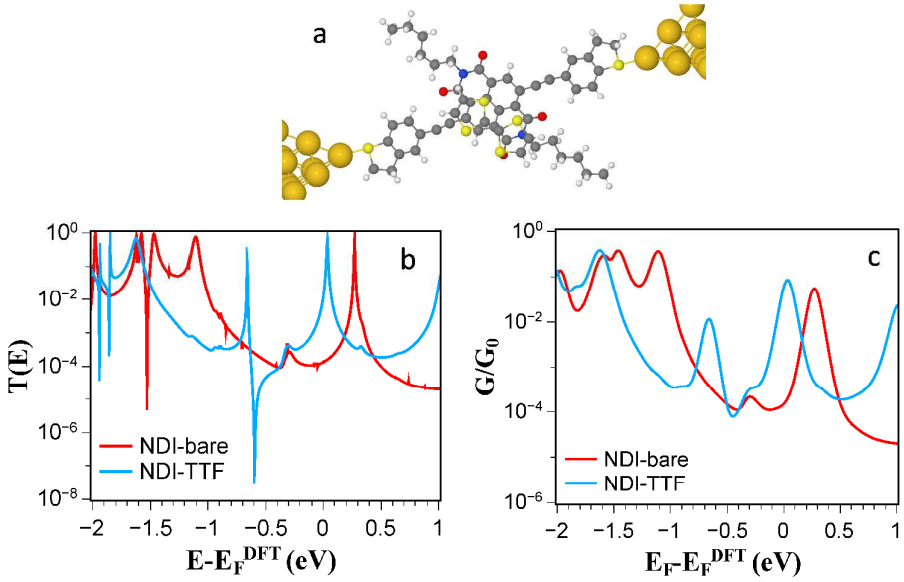

Figure 5. (a) An NDI molecule complexed with TTF. (b) Transmission coefficients as a function of energy for the NDI (red) and NDI-TTF (blue). (b) Room-temperature electrical conductance for the bare NDI (red) and NDI-TTF (blue).

Figure 5a shows that at $E-E_F^{DFT}$=-0.6eV, the interaction between a bound state on the TTF and the extended states of the NDI backbone produces a Fano resonance (ie a sharp resonance, accompanied by an anti-resonance) Figure 5 also shows that the TTF also shifts the position of the LUMO and HOMO resonances of NDI molecule to lower energies, reflecting the fact that (see Table 1) the TTF acts as a positively charged electrostatic gate. The Mott formula tells us that the Seebeck coefficient is proportional to the slope of the transmission coefficient *T(E)* at the Fermi energy and as demonstrated in Figure 5b, the shift from the undoped (red) transmission curve to the doped (blue) curve increases the slope at $E=E_F^{DFT}$, leading to an increase in the Seebeck coefficient at low temperatures, as shown in figure 6b. High-Seebeck coefficients after n-doping are not unprecedented in organic semiconductors. For example[28], Schlitz *et al.*[29] demonstrated that n-doping of napthalenedicarboximide-bithiophene copolymer P(NDIOD-T2) leads to a high negative Seebeck coefficient of $-850\ \mu V\ K^{-1}$. In contrast, calculations in the presence of TCNE (see SI) show that the latter acts as a negatively-charged electrostatic gate and shifts molecular resonances to higher energies. In this case, the doping is unfavourable, because centre of the HOMO-LUMO gap is shifted towards the DFT-predicted Fermi energy, thereby lowering the slope of *T(E)* and the value of the Seebeck coefficient relative to the bare NDI.

Table 1: DFT results for the number ΔN of electrons transferred from the TTF, the binding energy ΔE of the TTF to the NDI molecule and optimal distance of the TTF from the NDI.

	ΔN	*ΔE (eV)*	*D (Å)*
TTF	0.322	-0.807	3.25

Figure 6 shows the resulting Seebeck coefficients *S* and power factors σS^2 of bare and TTF-doped NDI. Figures 6a and 6c show results for a range of Fermi energies E_F relative to the DFT-predicted Fermi energy E_F^{DFT}, whereas Figures 6b and 6d show the corresponding results for a range of temperature, evaluated at the DFT Fermi energy. Figure 6b show that NDI with TTF have the highest power factor of 3.6×10^{-4} W/m.K^2. As shown in the SI, in the TCNE-doped NDI, LUMO resonance is shifted outward DFT Fermi energy and therefore both thermopower and electrical conductance is reduced in the vicinity of the DFT-predicted Fermi energy. Therefore, to obtain full ZT, we consider TTF-doped NDI by calculating the phonon contribution to thermal conductance.

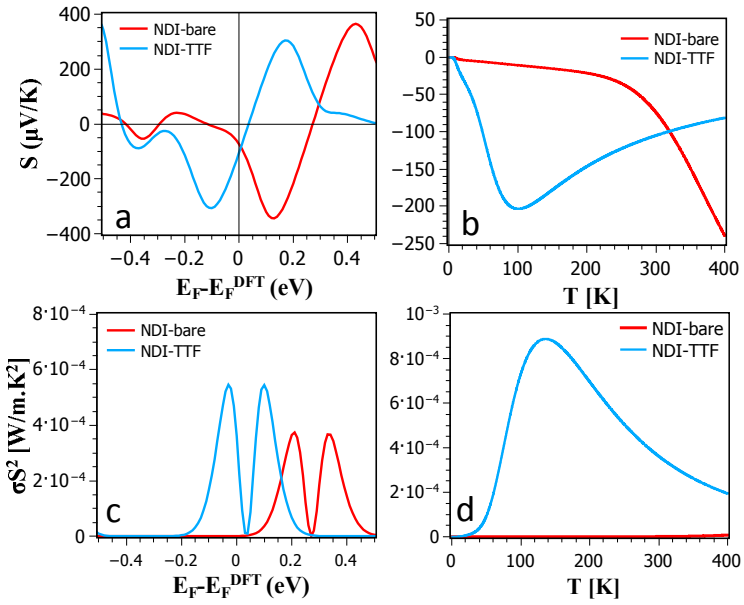

Figure 6. (a) and (c) Room-temperature Seebeck coefficients and power factors versus Fermi energy for bare and TTF-doped NDI. (b) and (d) Seebeck coefficients and power factors versus temperature, evaluated using the DFT-predicted value of the Fermi energy.

Following the method in[6], we calculate the vibrational properties of the bare NDI and TTF-doped NDI by constructing the dynamical matrix $D_{ij} = \left(F_i^q(\delta q_j') - F_j^q(-\delta q_j')\right)/2M_{ij}\,\delta q_j'$ where F and M are the force and mass matrices and $\delta q' = 0.01$ Å is each atom displacement from optimised geometry in positive and negative x, y, and z directions. For a molecule within a junction, the dynamical matrix describes an open system composed of the molecule and two semi-infinite electrodes and is used to calculate the phonon transmission coefficient $T_{ph}(\omega)$ for phonons with energy $\hbar\omega$ passing through the bare NDI and TTF-doped NDI from the right to the left electrodes as shown in Figure 7.

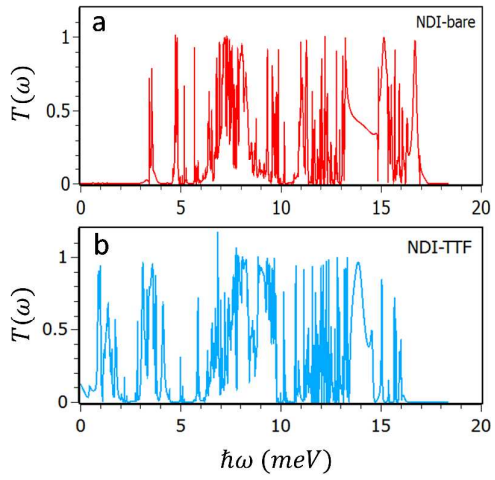

Figure 7. Phonon transmission coefficients for bare and TTF-doped NDI.

The thermal conductance due to the phonons could be calculated from the phononic transmission coefficient $T_{ph}(\omega)$ as: $\kappa_{ph}(T) = \frac{1}{2\pi}\int_0^\infty \hbar\omega T_{ph}(\omega)\frac{\partial f_{BE}(\omega,T)}{\partial T}\, d\omega$ where $f_{BE}(\omega,T)$ is Bose−Einstein distribution function. From the phonon and electron transmission coefficients of figure 7 and 5 respectively, we obtain the phonon and electron contributions to the thermal conductance shown in figure 8.

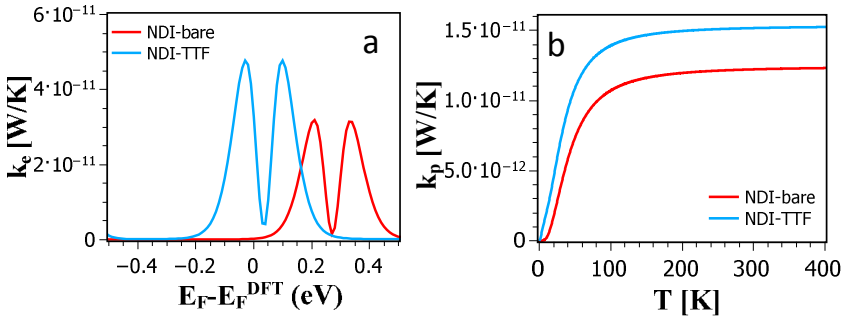

Figure 8. Electron and phonon contributions to the thermal conductance of bare and TTF-doped NDI.

When added together to yield the total thermal conductance, these results combine with those of figures 5 and 6 to yield the thermoelectric figure of merit ZT shown in figure 9, which reveals that in the presence of TTF doping, for Fermi energies within 0.1eV of the DFT-value, a ZT of order 1.2 is achievable.

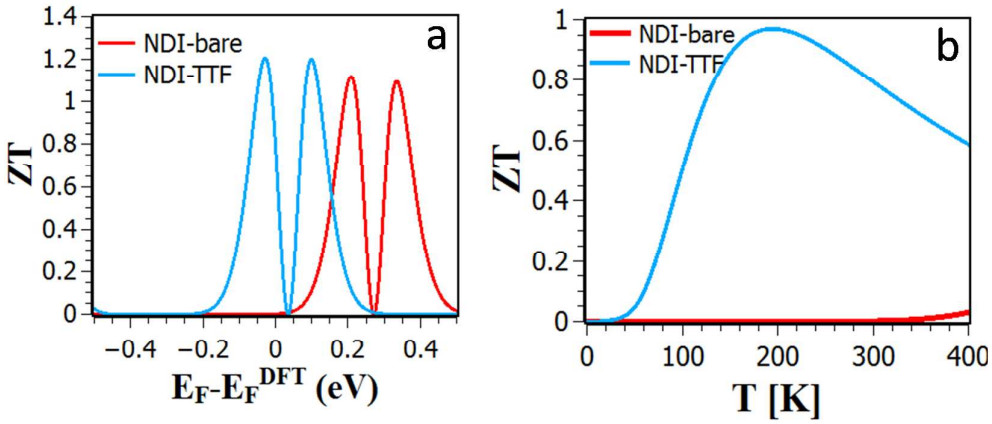

Figure 9. (a) Room-temperature ZT versus Fermi energy for bare and TTF-doped NDI. (b) ZT versus temperature evaluated using the DFT-predicted value of the Fermi energy.

In conclusion, to illustrate the advantages of using redox-active molecules in the design of thermolectric materials, we first studied the thermoelectric properties of NDI single-molecule junctions under electrochemical gating. The effect of an electrochemical gate is modelled by placing a charge double layer around the NDI and varying the distance of the charge double layer from the NDI backbone to control the charge state of the NDI. We predict that the three NDI charge states possess distinct thermoelectric properties. In particular the Seebeck coefficients of the neutral state are negative, whereas the anion and di-anion states possess a positive Seebeck coefficient.

Building upon this strategy for tuning thermoelectric properties, we also investigated the effect on both phonon and electron transport of doping the NDI with either an electron donor (TTF) or an electron acceptor (TCNE). We find that doping by TTF increases the room-temperature Seebeck coefficient and power factor from -73.66 μv/K and 2.6×10^{-7} W/m.K^2 for bare NDI to -105 μv/K and 3.6×10^{-4} W/m.K^2 in presence of TTF. The low thermal conductance of NDI-TTF, combined with the higher Seebeck coefficient and higher electrical conductance lead to a maximum thermoelectric figure of merit of ZT = 1.2, which is higher than that of NDI-bare in several orders of magnitude. This demonstrates that both the sign and magnitude of NDI Seebeck coefficient can be tuned reversibly by electrochemical gating and doping, suggesting that with appropriate doping, such redox active molecules are attractive materials for ultra-thin-film thermoelectric devices.

Methods

Transport formulae. In the linear-response regime, the electric conductance G and Seebeck coefficient S of a single-molecule junction are given by[24]

$$G = \frac{e^2}{h}L_0 \qquad (1)$$

$$S = \frac{1}{eT}\frac{L_1}{L_0} \qquad (2)$$

where T is the temperature. In these equations, the moments L_0 and L_1 are given by $L_n = L_n^{\uparrow} + L_n^{\downarrow}$ $(n = 0, 1)$, where

$$L_n^{\sigma} = \int_{-\infty}^{\infty} (E - E_F)^n \, T^{\sigma}(E) \left(-\frac{\partial f(E,T)}{\partial E}\right) dE \qquad (3)$$

In this expression, $\boldsymbol{T^{\sigma}(E)}$ is the transmission coefficient for electrons of energy $\boldsymbol{E}$, spin $\boldsymbol{\sigma}$ = [↑, ↓] passing through the molecule from one electrode to the other and $\boldsymbol{f(E,T)}$ is Fermi distribution function $\boldsymbol{f(E,T) = [\exp(\frac{E-E_F}{k_B T}) + 1]^{-1}}$, where $\boldsymbol{k_B}$ is Boltzmann's constant. For $\boldsymbol{E}$ close to the Fermi energy $\boldsymbol{E_F}$, if $\boldsymbol{T(E)}$ varies only slowly with $\boldsymbol{E}$ on the scale of k_BT then these formulae take the form:

$$G(T) \approx \left(\frac{2e^2}{h}\right) T(E_F), \qquad (4)$$

$$S(T) \approx -\alpha e T \left(\frac{d\, lnT(E)}{dE}\right)_{E=E_F}, \qquad (5)$$

where $\boldsymbol{\alpha = \left(\frac{k_B}{e}\right)^2 \frac{\pi^2}{3}}$ =2.44 10^{-8} WΩK^{-2} is the Lorentz number. Equation (5) demonstrates that the sign and value of $\boldsymbol{S}$ is tuned by changing the slope of ln $\boldsymbol{T(E)}$ near $\boldsymbol{E = E_F}$ and hence it is of interest

to explore whether or not the ability to vary the charge states of *NDI* can be used to control thermoelectricity.

Density Functional Theory To compute the moments L_n of the transmission coefficient of the NDI-based single-molecule junction shown in Figures 1 and 2, the following method was applied. First the relaxed geometry of molecule was found using the density functional (DFT) code SIESTA[30], which employs Troullier-Martins pseudopotentials to represent the potentials of the atomic cores[31], and a local-atomic-orbital basis set. A double-zeta polarized basis set was used for all atoms and the generalized gradient approximation (GGA-PBE) for the exchange and correlation functionals[32]. For the geometry optimization, the Hamiltonian and overlap matrix elements were calculated on a real-space grid defined by a plane-wave cutoff of 150 Ry and the NDI molecule was relaxed until the forces on the atoms were smaller than 0.02 eV/Å.

After obtaining the relaxed geometry of the isolated NDI molecule, we constructed the single-molecule junction by placing the optimized NDI molecule between gold electrodes as shown in Figure 1. After re-optimising the geometry, charge double layers were added to both sides of the planar backbone of the molecule following the technique describing in ref[22] and *T(E)* was calculated for each realisation of the double layer. The electron and spin transport calculations were performed with the GOLLUM transport code[33], which uses the DFT-generated mean-field Hamiltonian to compute the transmission coefficient *T(E)* for electrons of energy E passing from the left gold electrode to the right electrode. For the transport calculation, the Hamiltonian and overlap matrices were calculated with SIESTA, using DZP basis sets for all elements except gold, for which a DZ basis set was used, a GGA-PBE exchange-correlation parameterization. To describe accurately singly-occupied levels of the NDI all calculations were spin-polarized and the electron transmission coefficient function *T(E)* was calculated as the average of the spin up and spin down transmission coefficients.

Acknowledgment

This work is supported by the UK EPSRC, EP/K001507/1, EP/J014753/1, EP/H035818/1, and from the EU ITN MOLESCO 606728 and the Ministry of Higher Education and Scientific Research, Al Qadisiyah University, IRAQ.

Notes and References

1 C. Gayner and K. K. Kar, *Prog. Mater. Sci.*, 2016, **83**, 330–382.
2 X. Zhang and L.-D. Zhao, *J. Mater.*, 2015, **1**, 92–105.
3 X. F. Zheng, C. X. Liu, Y. Y. Yan and Q. Wang, *Renew. Sustain. Energy Rev.*, 2014, **32**, 486–503.
4 I. D. Hicks; M. S. Dresselhaus, *Phys. Rev. B*, 1993, **47**, 8–11.
5 L. D. Hicks and M. S. Dresselhaus, *Phys. Rev. B*, 1993, **47**, 727–731.
6 H. Sadeghi, S. Sangtarash and C. J. Lambert, *Nano Lett.*, 2015, **15**, 7467–7472.
7 K. Xu, P. Cao and J. R. Heath, *Nano Lett.*, 2009, **9**, 4446–4451.
8 H. Sadeghi, S. Sangtarash and C. J. Lambert, *Sci. Rep.*, 2015, **5**, 9514.
9 L. Rincón-García, C. Evangeli, G. Rubio-Bollinger and N. Agraït, *Chem. Soc. Rev.*, 2016.
10 H. Sadeghi, S. Sangtarash and C. J. Lambert, *2D Mater.*, 2017, **4**, 15012.
11 C. Evangeli, K. Gillemot, E. Leary, M. T. González, G. Rubio-Bollinger, C. J. Lambert and N. Agraït, *Nano Lett.*, 2013, **13**, 2141–2145.
12 Y. Nonoguchi, K. Ohashi, R. Kanazawa, K. Ashiba, K. Hata, T. Nakagawa, C. Adachi, T. Tanase and T. Kawai, *Sci Rep*, 2013, **3**, 3344.
13 Q. H. Al-Galiby, H. Sadeghi, L. A. Algharagholy, I. Grace and C. Lambert, *Nanoscale*, 2016, **8**, 2428–2433.
14 J. P. Small, K. M. Perez and P. Kim, *Phys. Rev. Lett.*, 2003, **91**, 256801.

15 O. Bubnova, M. Berggren and X. Crispin, *J. Am. Chem. Soc.*, 2012, **134**, 16456–16459.
16 H. Ohta, T. Mizuno, S. Zheng, T. Kato, Y. Ikuhara, K. Abe, H. Kumomi, K. Nomura and H. Hosono, *Adv. Mater.*, 2012, **24**, 740–744.
17 S. F. Svensson, A. I. Persson, E. A. Hoffmann, N. Nakpathomkun, H. A. Nilsson, H. Q. Xu, L. Samuelson and H. Linke, *New J. Phys.*, 2012, **14**, 0–11.
18 Y. Tian, M. R. Sakr, J. M. Kinder, D. Liang, M. J. MacDonald, R. L. J. Qiu, H. J. Gao and X. P. A. Gao, *Nano Lett.*, 2012, **12**, 6492–6497.
19 M. C. Llaguno, J. E. Fischer, A. T. Johnson and J. Hone, *Nano Lett.*, 2004, **4**, 45–49.
20 P. M. Wu, J. Gooth, X. Zianni, S. F. Svensson, J. G. Gluschke, K. A. Dick, C. Thelander, K. Nielsch and H. Linke, *Nano Lett.*, 2013, **13**, 4080–4086.
21 Y. M. Zuev, W. Chang and P. Kim, *Phys. Rev. Lett.*, 2009, **102**, 1–4.
22 Y. Li, M. Baghernejad, A. G. Qusiy, D. Zsolt Manrique, G. Zhang, J. Hamill, Y. Fu, P. Broekmann, W. Hong, T. Wandlowski, D. Zhang and C. Lambert, *Angew. Chemie - Int. Ed.*, 2015, **54**, 13586–13589.
23 C. J. Lambert, *Chem. Soc. Rev.*, 2015, **44**, 875–888.
24 C. J. Lambert, H. Sadeghi and Q. H. Al-galiby, *Comptes Rendus Phys.*, 2016, **1**, 1–12.
25 A. Shakouri and S. Li, *Thermoelectr. 18th ICT*, 1999, 402–406.
26 H. Shi, C. Liu, J. Xu, H. Song, Q. Jiang, B. Lu, W. Zhou and F. Jiang, *Int. J. Electrochem. Sci.*, 2014, **9**, 7629–7643.
27 M. Sumino, K. Harada, M. Ikeda, S. Tanaka, K. Miyazaki and C. Adachi, *Appl. Phys. Lett.*, 2011, **99**, 93308.
28 R. Kroon, D.A. Mengistie, D. Kiefer, J. Hynynen, J.D. Ryan, L. Yu, C. Muller, C., *Chem. Soc. Rev.* 2016, **45**, 6147-6164
29 R. A. Schlitz, F. G. Brunetti, A. M. Glaudell, P. Levi Miller, M. A. Brady, C. J. Takacs, C. J. Hawker and M. L. Chabinyc, Adv. Mater. 2014, **26**, 2825–2830
30 J. M. Soler, E. Artacho, J. D. Gale, A. Garcia, J. Junquera, P. Ordejon and D. Sanchez-Portal, *J. physics. Condens. matter* , 2002, **14**, 2745.
31 N. Troullier and J. L. Martins, *Phys. Rev. B*, 1991, **43**, 8861–8869.
32 J. P. Perdew, K. Burke and M. Ernzerhof, *Phys. Rev. Lett.*, 1997, **78**, 1396–1399.
33 J. Ferrer, C. J. Lambert, V. M. García-Suárez, D. Z. Manrique, D. Visontai, L. Oroszlany, R. Rodríguez-Ferradás, I. Grace, S. W. D. Bailey, K. Gillemot, H. Sadeghi and L. A. Algharagholy, *New J. Phys.*, 2014, **16**, 93029.

Supporting Information

Tuning the Seebeck coefficient of naphthalenediimide by electrochemical gating and doping

Qusiy H. Al-Galiby,[a,b*], Hatef Sadegi,[a] David Zsolt Manrique,[c] and Colin J. Lambert[a*]

[a]Department of Physics, Lancaster University, Lancaster LA1 4YB, United Kingdom.
[b]Department of Physics, Education of College, Al Qadisiyah University, IRAQ.
[c]Department of Electronic & Electrical Engineering - Photonics Group, University College London, United Kingdom.

*Corresponding author: c.lambert@lancaster.ac.uk and qusiy.algaliby@qu.edu.iq

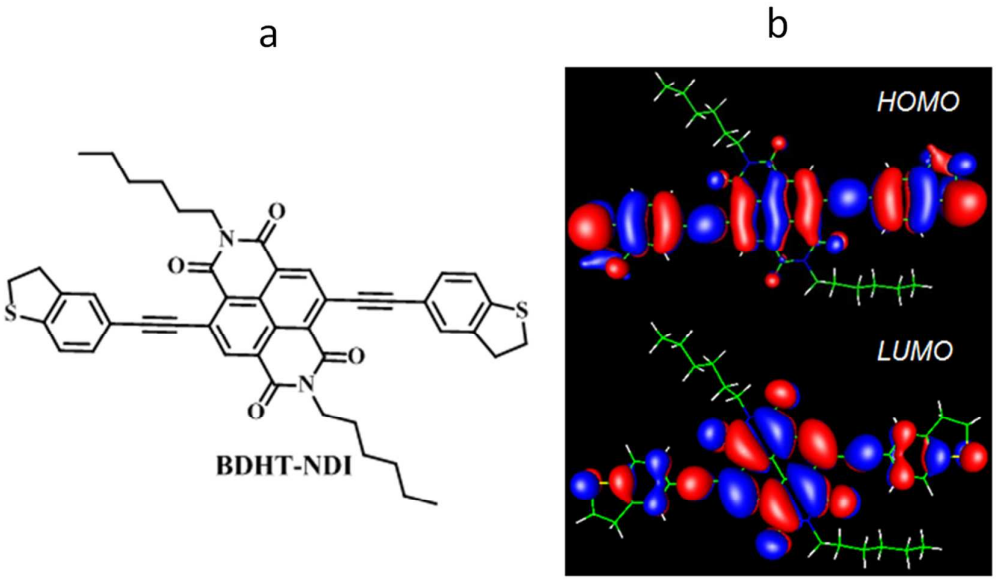

Figure S1. The left figure 1a shows the chemical structure of BDHT-NDI molecule, the right figure 1b shows Iso-surfaces of frontier molecular orbitals of NDI molecule obtained using DFT. Red corresponds to positive and blue to negative regions of the wave functions.

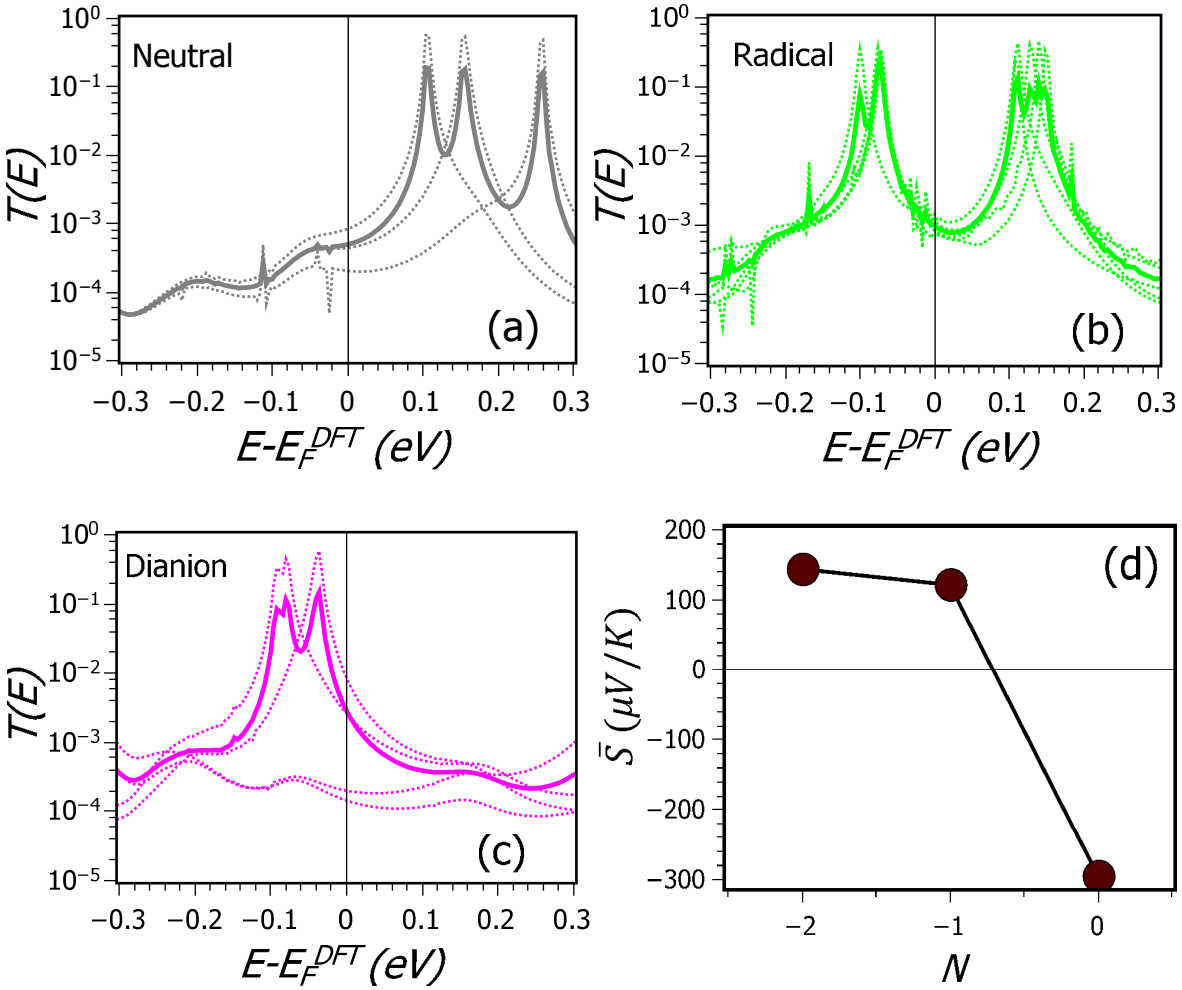

Figure S2. (a) Transmission curves for junction geometries with double layers located at distances y=5Å, y=5.8Å and y=4.05Å, respectively. The continuous curves are the averaged transmission coefficients $\bar{T}(E)$ and the dotted curves show the transmission coefficients for different charge double layer arrangements. Figure 4d shows the average room-temperature thermopower $\bar{S}$ for three redox states obtained using DFT-predicted Fermi energy E_F^{DFT}. The colour code refers to the three different states, NDI-N (black), NDI-R (blue) and NDI-D (red).

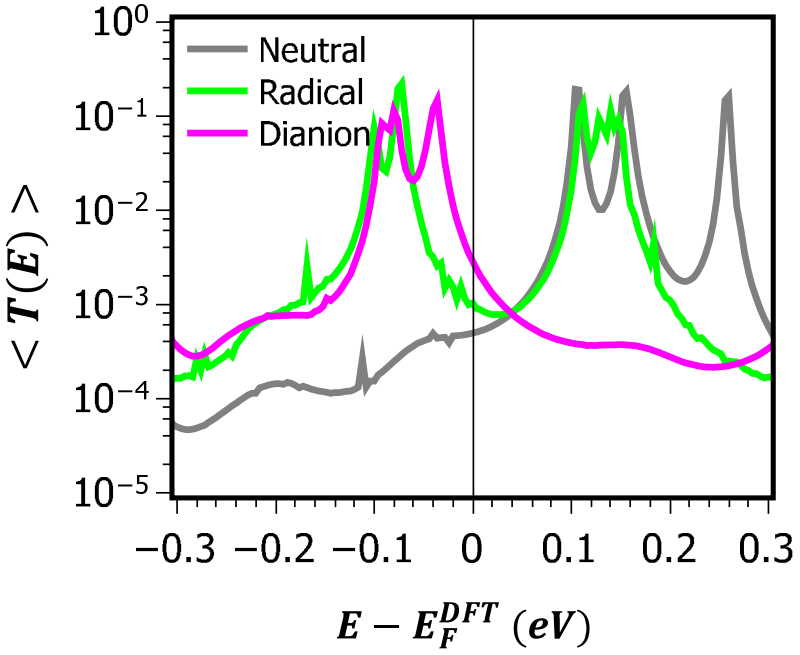

Figure S3. The corresponding ensemble-averaged tranmsission coefficients corresponding to Figure 3 of the main text

NDI doping with TTF:

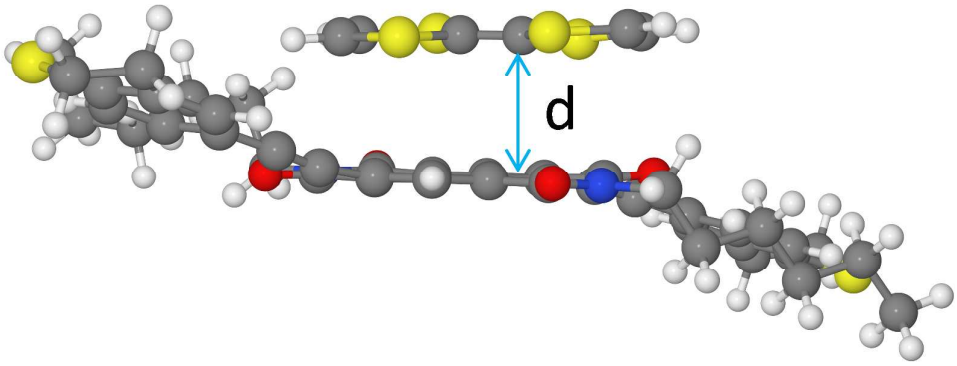

Figure S4: Optimised configurations for TTF bonded to the NDI molecule.

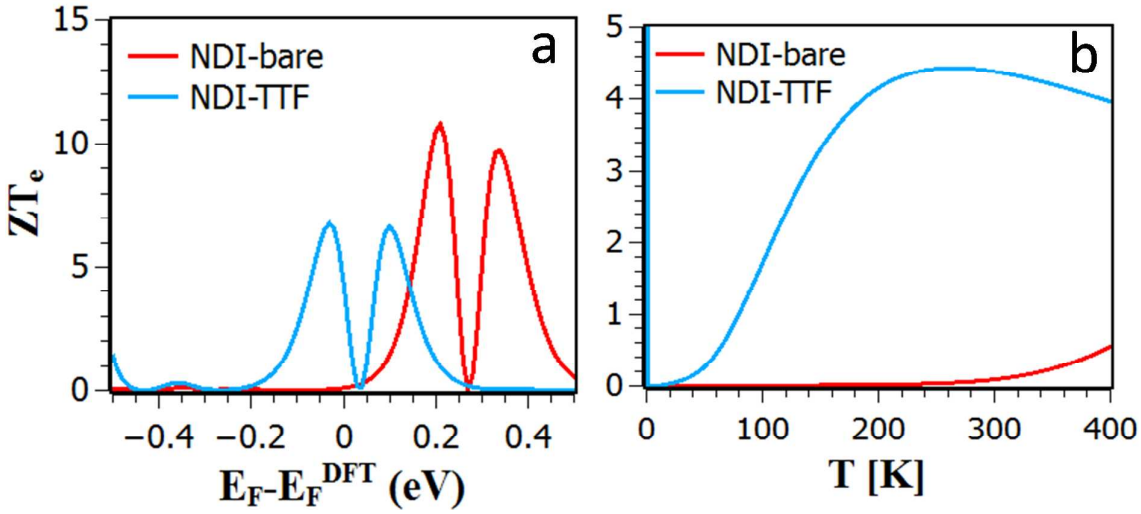

Figure S5. (a) Room-temperature- electronic contribution to figure of merit ZT_e versus Fermi energy for bare and TTF-doped NDI. (b) Electronic contribution to figure of merit ZT_e versus temperature, evaluated using the DFT-predicted value of the Fermi energy.

NDI doping with TCNE:

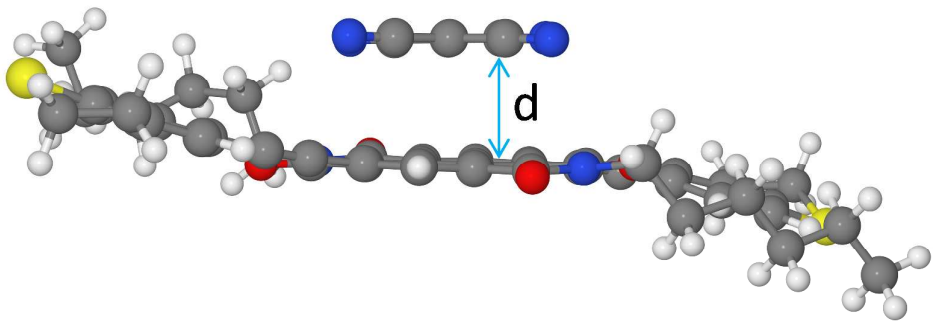

Figure S6: Optimised configurations for TCNE bonded to the NDI molecule.

Table S1: DFT results for the number ΔN of electrons transferred to the TCNE, the binding energy ΔE of the TCNE to the NDI molecule and optimal distance of the TCNE from the NDI.

	ΔN	*ΔE (eV)*	*D (Å)*
TCNE	-0.217	-0.288	3.85

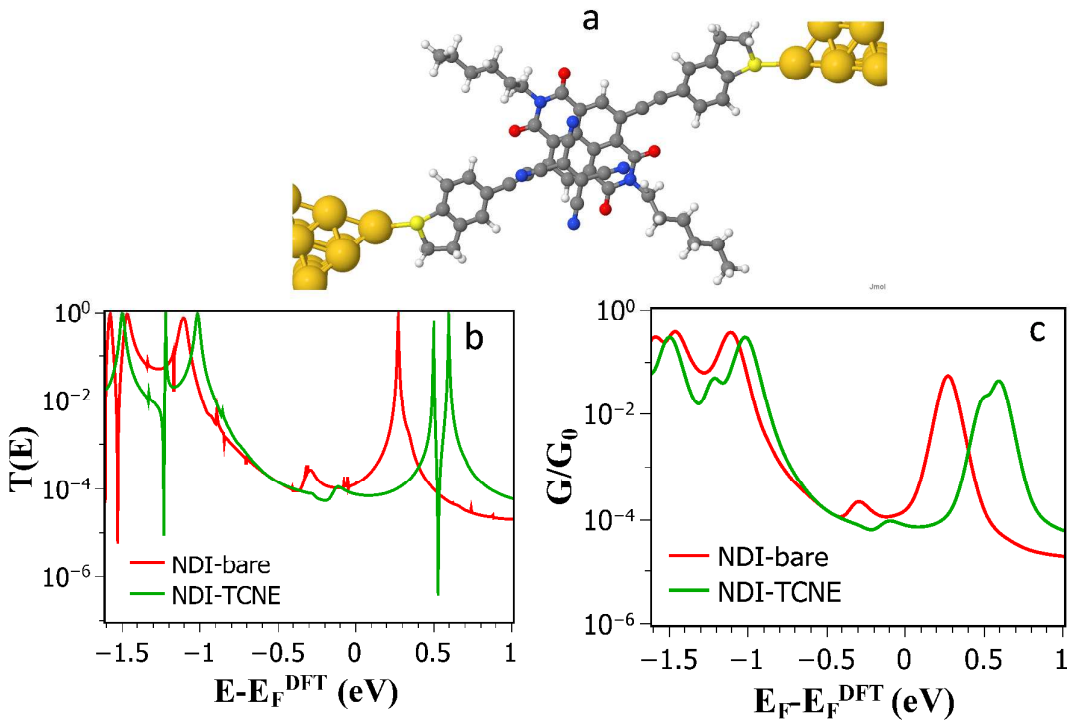

Figure S7. (a) An NDI molecule complexed with TCNE. (b) Transmission coefficients as a function of energy for the NDI (red) and NDI-TCNE (green). (b) Room-temperature electrical conductance for the bare NDI (red) and NDI-TCNE (green).

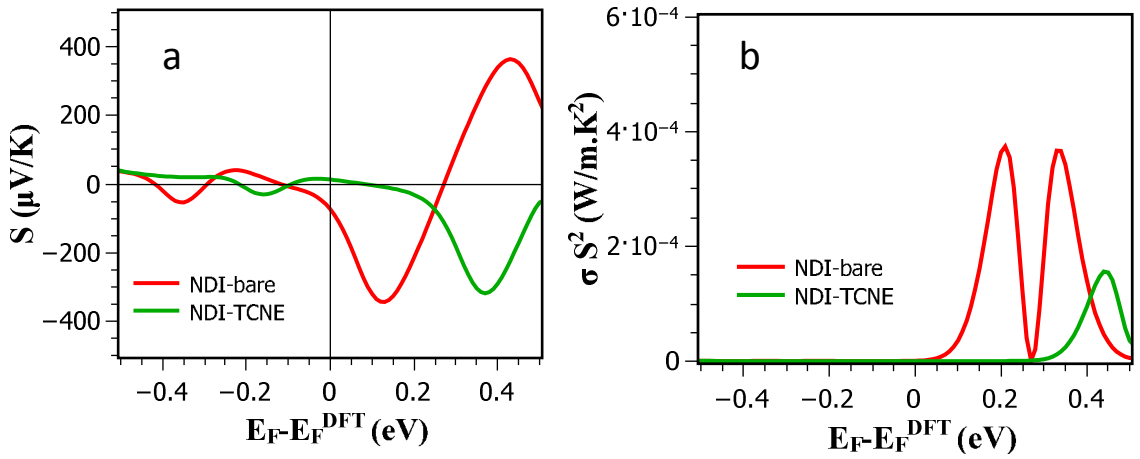

Figure S8. Room-temperature Seebeck coefficients and power factors versus Fermi energy for bare and TCNE-doped NDI.